PCCP

Accepted Manuscript

ROYAL SOCIETY OF CHEMISTRY

www.rsc.org/pccp

Theoretical Design of the Cyclic Lipopeptide Nanotube as a Molecular Channel in the Lipid Bilayer, Molecular Dynamics and Quantum Mechanics Approach

Mohammad Khavani, Mohammad Izadyar*, Mohammad Reza Housaindokht

Department of Chemistry, Faculty of Sciences, Ferdowsi University of Mashhad, Mashhad, Iran

izadyar@um.ac.ir

Telefax: +985138795457

Abstract

In this article, cyclic peptide (CP) with lipid substitutions were theoretically designed. Dynamical behavior of the CP dimers and cyclic peptide nanotube (CPNT) without lipid substitutions in the solution (water and chloroform) during the 50 ns molecular dynamic (MD) simulations has been investigated. As a result, the CP dimers and CPNT in non-polar solvent are more stable than polar solvent and CPNT is a good container for non-polar small molecules such as chloroform. The effect of the lipid substitutions on the CP dimers and CPNT has been investigated in the next stage of our studies. Accordingly, these substitutions increase the stability of the CP dimers and CPNT, significantly, in polar solvents. MM-PBSA and MM-GBSA calculations

confirm that substitution has an important effect on the stability of the CP dimers and CPNT. Finally, dynamical behavior of CPNT with lipid substitutions in fully hydrated DMPC bilayer shows a high ability of this structure, for molecule transmission across the lipid membrane. This structure is enough stable to be used as a molecular channel.

DFT calculations on the CP dimers in the gas phase, water and chloroform, indicate that H-bond formation is the driving force for dimerization. CP dimers are more stable in the gas phase in comparison to solution. HOMO-LUMO orbital analysis indicate that the interaction of the CP units in the dimer structures is due to the molecular orbital interactions between the NH and CO groups.

Introduction

Cyclic peptide nanotubes (CPNTs) are a class of the synthetic proteins with many applications in different fileds[1-7] such as, biology, drug delivery, antimicrobial agent, electronics, optics and nanotechnology.[8-17] For example Fu and co-workers investigated the drug delivery ability of the CPNT by employing experimental and theoretical methods for transmission of 5-Fluorouracil antitumor drug across the lipid bilayer.[18] Also Subramanian and co-workers investigated the drug delivery ability of some CPNTs for drug transmission through the lipid

bilayer, too.[19] These studies indicate that CPNTs are a good choice for transmission of small drug molecules inside the cell membrane. Some cyclic hexapeptides which were synthesized by Schmieder[20] and co-workers, show an antimicrobial activity on the Gram-positive and negative bacteria.

Cyclic peptide is formed from the closed rings that have even number of alternating D- and L-amino acid residues. These structures can perch on top of each other and through the hydrogen bond formation produce a CPNT. Side chain nature of the cyclic peptide can determine the hydrophobic or hydrophilic properties of cyclic peptide.[1,2] Cyclic peptide nanotubes with hydrophobic side chains are in more attention than CPNTs with hydrophilic side chains, because the hydrophobic side chains have better compatibility with biological membranes.[21] CPNTs can have selective and efficient ion transport across the biological membrane.[22] For example, Granja and co-workers, by employing experimental and theoretical methods, showed that some CPNTs have selective ion transport of alkali or alkaline earth cations.[23]

As a result, some parameters such as amino acid composition and solvents have key roles on the stability of CPNTs and these structures are more stable in the non-polar solvents than polar ones.[24,25] For example Granja and co-workers, by molecular dynamic simulations, investigated the effect of the D-amino acid units on the stability of CPNT. [26] According to their results, CPNT with

cyclohexapeptide composed of cis-3-aminocyclohexanecarboxylic acid showed a better stability in polar and non-polar solvents. The stability of these structures is determined by the intermolecular hydrogen bond interaction between the cyclic peptides. Cyclic self-assembled peptides create a tubular structure in the lipid bilayer through the hydrogen bond formation. These hydrogen bond formation has been confirmed by FT-IR, molecular modeling and X-ray crystallography studies.[1,27]

In this article, CPNT formation from the cyclic peptides consisting of [-(L-Leu-D-^{Me}N-γ-Acp)$_4$-] (Scheme 1-A) and its derivatives have been investigated by molecular dynamic (MD) simulations and quantum mechanics calculations. We studied the solvent effects in water, chloroform and octadecanoic acid (stearic acid) as a lipid substitution (Scheme 1-B) on the stability of the cyclic peptide dimers and CPNT. Here, we presented the result of 50 ns MD simulations on these structures in water and chloroform and CPNTs behavior inside the dimyristoylphosphatidylcholine (DMPC) bilayer. Moreover to understand the cyclopeptide dimer behaviors, in the gas phase and solvents, DFT calculations, natural bond orbital analysis (NBO) and quantum theory of atoms in molecules (QTAIM) have been performed.

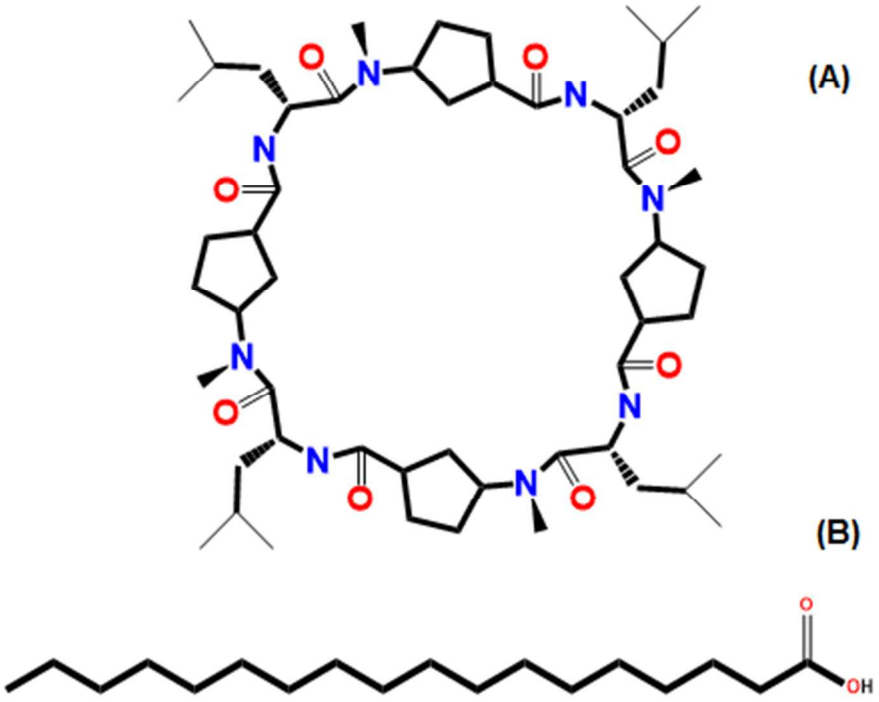

Scheme 1. (A) Single cyclic peptide composed of [-(L-Leu-D-^{Me} N-γ-Acp)$_4$-] and (B) stearic acid.

Methods

Molecular dynamic simulation details

Five systems which composed of the cyclic peptide (CP) have been simulated and studied in this work. Simulated systems were denoted as CPNT and D for the cyclic peptide nanotube and dimer, respectively. The atomic coordinates of the CP which are composed of [-(L-Leu-D-^{Me} N-γ-Acp)$_4$-] (Scheme 1-A) were obtained from a previous X-ray crystal structure.[28] Where Acp corresponds to the cis-3-aminocyclopantanecarboxilic acid. This CP1 can produce only the dimer structure (CP1D) according to the experimental results.[28] CP2 and its dimer are

made of CP1 with the exception that the connected methyl groups to nitrogen atom were substituted by hydrogen atoms. A tubular ensemble composed of ten CP2s was chosen as the CPNT1. CH_2—$CH(CH_3)_2$ groups of the leucine amino acids of CPNT1 were substituted by stearic acid (Scheme 1-B) as a lipid substitution abbreviated as CPNT2. Since the stearic acid is normally in an ionic form, H atom of OH groups of this substitution has been removed in CPNT2. The cyclic peptide nanotube within the ionic lipid substitution demonstrates as CPNT3.

At the first step of MD simulations, energy minimization in an implicit solvent environment has been performed on the dimers and CPNTs structures to reduce unfavorable short contacts. Then each structure was solvated explicitly with a cubic box of water and chloroform molecules extended 15 Å away from the solute. Water and chloroform molecules were simulated using the TIP3P and AMBER force field, respectively.[29-32] Energy minimization on the structures in water and chloroform has been performed during 30000 steps. After this step, each system was heated in an NVT ensemble from 0 to 300 K during 200 ps by employing typical values of the restraining force constant of 1000 kJ mol^{-1} nm^2 for solute structures. Obtained structures of this step were used for equilibration step in an NPT ensemble (at 300 K and 1 bar) during the 200 ps without any positional restraints. Finally, the results of the equilibration step were used for 50 ns MD simulations (product step) in the NPT ensemble by using the 2 fs time step. The

membrane model was constructed from the fully hydrated DMPC bilayers containing 200 lipid units. CPNT1 and CPNT3 were inserted in the center of the bilayer with its long axis normal to the interface. When CPNTs inserted inside the DMPC bilayer, 53 K^+ within 13 Cl^- and 20 K^+ within 20 Cl^- ions were added to the systems for CPNT3 and CPNT1, respectively. Minimization, heating, equilibration and product steps of the CPNT1 and CPNT3 inside the DMPC bilayer are as the same conditions that were reported for all structures without DMPC bilayer.

Temperature and pressure in the NPT MD simulations were controlled by a Langvin thermostat[33,34] with a collision frequency of 2 ps^{-1} and relaxation time of 1 ps for temperature and pressure, respectively. A time step of 2 fs was used throughout with the SHAKE constraint on all bonds involving hydrogen atoms.[35] In the calculation of the long-rang electrostatic interaction, the Particle Mesh Ewald method (PME)[36] with 8 Å direct space cut-off has been employed. All MD simulations have been performed by using the AMBER 12.0 simulation software package.[37] FF12SB[38], Lipid14[39] and general Amber force fields (GAFF)[40] have been employed for the cyclic peptides, DMPC bilayer and all derivatives respectively.

Free energy of binding for the addition of each CP to other CP units was calculated using the molecular mechanics-Poisson-Boltzmann surface area (MM-PBSA) and molecular mechanics-Generalized-Born surface area (MM-GBSA)

methods by using AMBER Tools 13.0. [25, 41-44] In the calculation of the free energies of binding for each CP unit of the CPNTs, production MD simulations was performed for 2 ns with a time step of 2 fs for the CPNTs with 2 to 10 units (minimization, heating and equilibration steps are the same as previous conditions). The details of MM-PBSA and MM-GBSA calculations were described in our previous study.[24]

DFT calculation details

Density functional theory (DFT) calculations have been employed for investigation of the dimerization process of CP1 and CP2 in the gas phase, water and chloroform. The structures of the monomers and the dimers of the CP1 and CP2 were optimized using the M05-2X functional[45] by employing 6-31G(d) basis set[46] as implemented in Gaussian 09 software.[47] Vibrational frequencies were calculated, to provide an estimation of the zero point energies (ZPEs) and the effect of dimerization on the N—H and C=O vibrational modes and hydrogen bonds. The conductor-like polarizable continuum model (CPCM)[48,49] was applied for investigation of the effect of water and chloroform on the molecular descriptions. To calculate the electronic charge changes and donor-acceptor interactions process natural bond orbital (NBO) analysis was applied.[50] Finally, the topological properties,[51,52] electron location function (ELF), localized orbital locator (LOL)[53-59] and atoms in molecules (AIM)[51] analyses were performed for

investigation the H-bond formation inside the CP dimers. All these analyses have been performed by MultiWFN 3.1 program.[60]

Results and discussion

MD simulation results

The stability of CP1D and CP2D in water and chloroform

Dynamical behavior of CP1 and CP2 dimeric nanotubes in the water (as a polar solvent) and chloroform (as a non-polar solvent) during the 50 ns MD simulations have been investigated. According to the experimental data, CP1 makes only a dimer structure in a solution mixture[28], while in the case of CP2 methyl groups were substituted by a hydrogen atom in order to investigate the possibility of the self-assembling, in water and chloroform during the 50 ns MD simulations.

Root mean square deviation (RMSD) values of the CP1D in chloroform and water during the 50 ns MD simulations have been calculated and shown in Figure 1-C. According to this figure, the maximum values of RMSD for the CP1D in the water and chloroform are 2.4 and 2.3 Å, respectively. These values are too small and shows the enough stability of CP1D in these solvents. Analysis of the radii of gyration (Rg) of CP1D (Figure 1-D) during the MD simulations confirmed the RMSD results and reveals the high stability of CP1D. The average distance

between the N and O atom of CP1D after 50 ns MD simulations in water and chloroform are 3.01 and 2.86 Å, respectively. These values are near to the distance between these atoms in the X-ray crystal structure (2.93 Å). This result confirms the RMSD and Rg values and reveals the stability of CP1D in polar and non-polar solvents. According to calculation, the average number of H-bond (NH···O=C) between the CP1 monomers of CP1D in water and chloroform are 6 and 7, respectively, during the MD simulation. Since, water molecules compete with the CO and NH groups of CP1D for formation H-bond, the number of inter-subunits H-bond of CP1D in water is lower than chloroform. The average H-bond length is 2.06 Å in water, which is exactly equal to the distance between the O and H atoms in X-ray crystal structure[28]. The corresponding value in chloroform is 1.87 Å, which is lower than water. According to the results, higher number of H-bond, lower RMSD and Rg and shorter H-bond length, CP1D is more stable in chloroform than water. Figure 1 shows the obtained structures of CP1D in water (A) and chloroform (B) after 50 ns MD simulations. This figure shows the stable and the tubular structure of this dimer in these solvents. Figure S1 shows the partial distribution function of O···H pairs (NH···O=C) of CP1D in water and chloroform. This figure shows the probability of finding a pair of O···H in terms of intermolecular distance. According to this figure the first peak in water and chloroform which are near to each other are at r=1.86 and 1.85 Å, respectively.

This peak is related to the O···H distance, and confirms the H-bond formation between the CP1 monomer of CP1D.

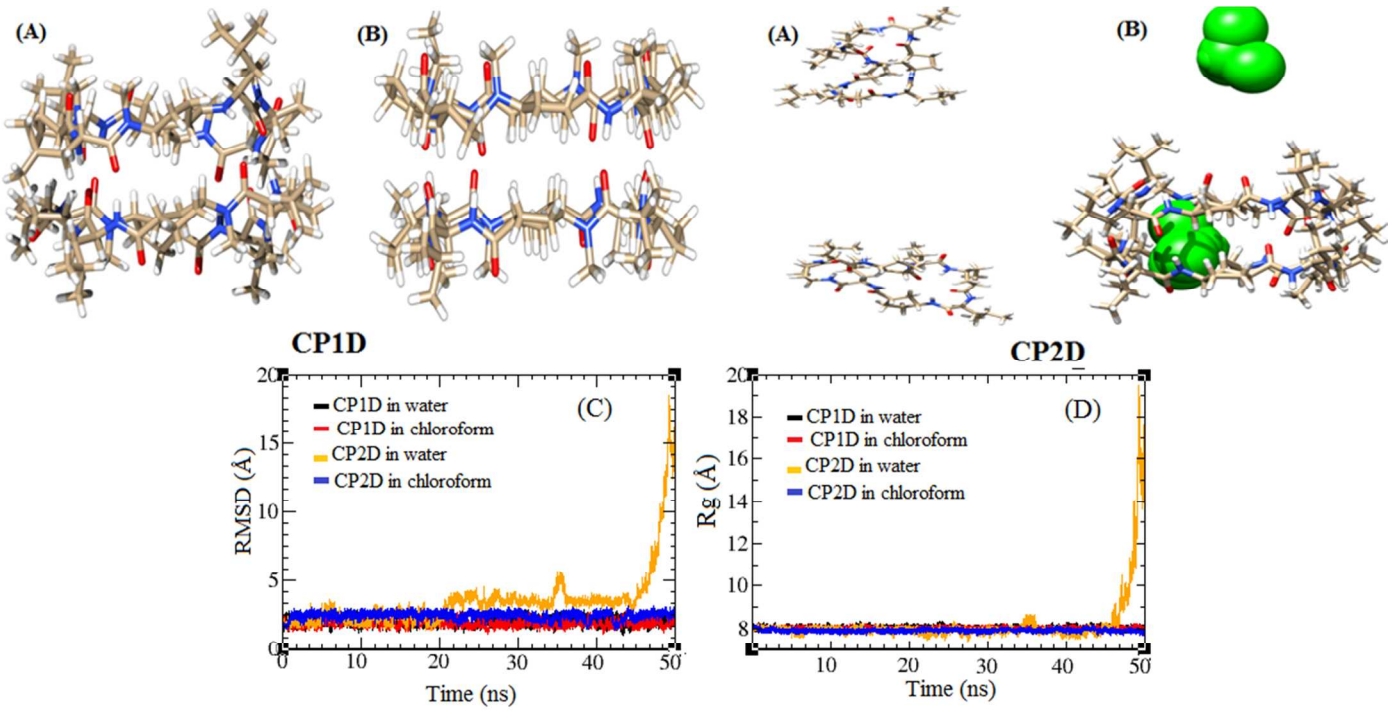

Figure 1. Obtained structures of CP1D and CP2D after 50 ns MD simulations in (A) water and (B) chloroform, and calculated (C) RMSD and (D) Rg values of the dimer structures during this MD simulation.

Figure 1 shows the obtained structures of CP2D after 50 ns MD simulations in water (A) and chloroform (B). According to this figure, CP2D is not stable in water while in chloroform shows a good stability. CP2 monomers are completely separated from each other in water, while CP2D is a stable dimeric tubular in the chloroform and chloroform molecule were trapped in its cavity. Calculated RMSD values of the CP2D (Figure 1-C) reveals that this structure is only stable in water during the 20 ns while in chloroform is completely stable. The maximum RMSD

value of this structure is 2.9 Å in chloroform. The analysis of Rg values confirmed the RMSD diagrams and higher values shows that CP2D is less compact in water in comparison to chloroform. The average number of H-bond of the CP2D is 7 in chloroform which is equal to the calculated value of CP1D in this solvent (because CP2D in water is not stable, the number of the H-bond was not included). Calculated average H-bond length in CP2D is 1.9 Å in chloroform, which is longer CP1D. Average distance of the N and O atoms of CP2D is 2.86 in chloroform which is equal to CP1D. Figure S1 shows the calculated RDF for O···H pair of CP2D in chloroform. According to this figure, the first sharp peak at 1.85 Å, equals to the calculated value for CP1D, indicates a similar and opposite behavior of CP1D and CP2D in the chloroform and water, respectively.

Dynamical behavior of the self-assembled peptide nanotube

For understanding the correlation of the stability and dynamical properties of the CPNT and the dimer structures, 50 ns MD simulations have been performed on the cyclic peptide nanotube composed of ten CP2 units (CPNT1) in water and chloroform. CP1 cannot form a CPNT structure according to experimental and theoretical data[28], because the methyl groups prevent the formation of H-bond between the CP units. Obtained structures of CPNT1 after 50 ns MD simulations are depicted in Figure 2, in water and chloroform. According to this figure, CPNT1 is not stable in water, while being too stable in chloroform. Since fourteen

molecules of chloroform out of fifty ones were trapped in the CPNT1 cavity after the MD simulation, it is reasonable to say that CPNT1 is a good container for non-polar molecules such as chloroform. Calculated RMSD values of CPNT1 in water and chloroform (Figure 2-C) confirm the stability of this structure in non-polar solvent. The maximum RMSD of this structure in chloroform is 1.6 Å, while the calculated RMSD values of CP1D and CP2D in chloroform are 2.3 and 2.9 Å, respectively. Calculated Rg values (Figure 2-D) of this structure reveal that CPNT1 in the chloroform is more compact than water. Root mean square fluctuation (RMSF) plots (Figure 2-E) show that the central parts of CPNT1 are more rigid while terminal parts are more flexible. Moreover, RMSF values indicate that increase in the number of the CP units of the CPNT1, decreases their stability, especially in the ninth and tenth monomers.

The amounts of the H-bonds as a function of the time during the 50 ns MD simulations, in water and chloroform were shown in Figure 3-B. Accordingly the amount of the H-bond in chloroform (62) slightly is more than in the water (45), therefore CPNT1 is more stable in non-polar solvent and has the lower RMSD values.

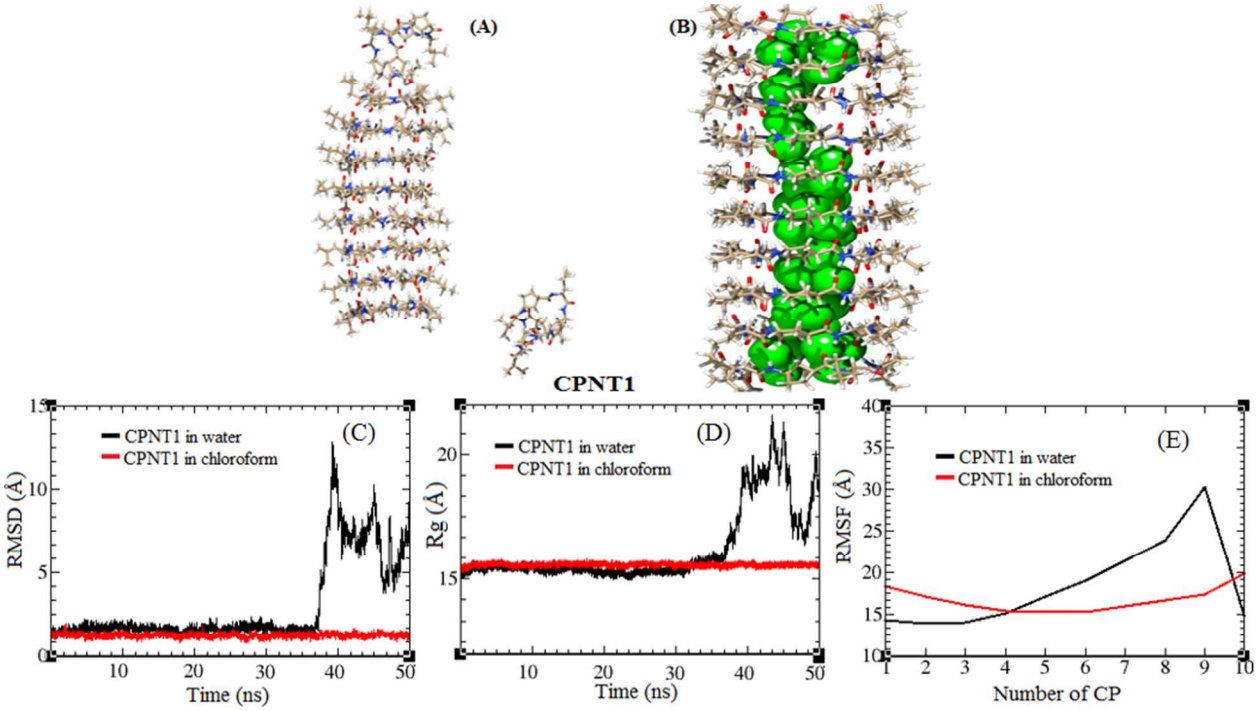

Figure 2. Obtained structures of the CPNT1 after the 50 ns MD simulations in (A) water and (B) chloroform. (C) RMSD, (D) Rg and (E) RMSF values of this structure in water and chloroform during the MD simulations.

Table 1 shows the average distance of the O (C=O) and N (NH) atoms in the CP units of the CPNT1 in water and chloroform. According to this table, the average distance is in the range of 2.90-3.28 and 2.79-3.02 Å in water and chloroform, respectively. These results reveal that the CP units of CPNT1 in chloroform are closer to each other than in water, which confirms the lower values of Rg for CPNT1 in chloroform. Average H-bond length (Table 1) of CPNT1 are in the range of 1.91-2.55 and 1.82-2.04 Å in water and chloroform, respectively. CPNT1 possesses lower RMSD and stable structure in chloroform due to more number of the H-bonds and their short length in this solvent.

Table 1. Calculated average distance between the N and O atoms and average H-bond length (Å) in water and chloroform for each CP monomer in the CPNT1.

	solvent	1-2	2-3	3-4	4-5	5-6	6-7	7-8	8-9	9-10
N⋯⋯O	Water	2.90	2.94	2.90	2.93	3.28	3.16	3.23	…..	…..
	chloroform	2.97	2.87	2.84	2.85	3.02	2.79	2.86	2.99	2.95
O⋯⋯H	Water	1.91	2.04	1.95	1.97	2.52	2.41	2.55	….	….
	chloroform	1.96	2.04	1.86	1.82	1.96	1.86	1.86	1.89	1.97

Calculated RDFs (Figure 3-A) of the O⋯H (C=O⋯NH) pair of the CPNT1 in water and chloroform show the sharp peaks at r=1.82 and 1.79 Å, respectively which confirms H-bond formation between the CP monomers of the CPNT1.

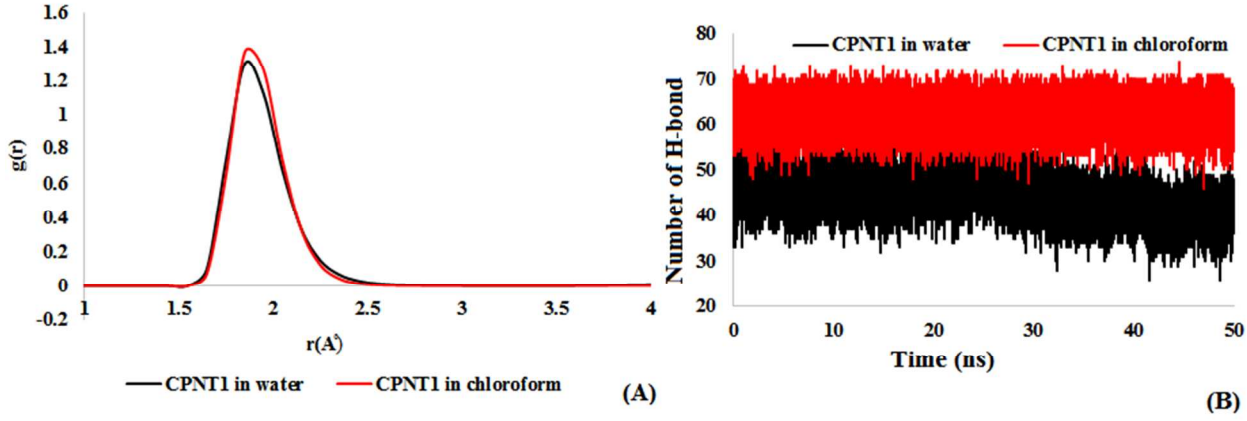

Figure 3. (A) Calculated RDF of the O⋯H pair and (B) the number of the H-bond during the 50 ns MD simulations of CPNT1 in water and chloroform.

The effect of lipid substitutions on the stability of the CP dimers and CPNT

According to the obtained results, CP dimers and CPNT1 are more stable and have a longer length in the non-polar solvent. Therefore the effect of the lipid substitutions (stearic acid) on the stability and the length of these nanostructures is of interest in water and chloroform.

Figure 4 shows the CP1D structures with lipid substitutions in water (A) and chloroform (B) after 50 ns MD simulations. Accordingly CP1D substituted by lipid has a tubular structure in both of the solvents and these substitutions are closer to each other and more compact in water. Calculated RMSD values for the central heavy atoms of the CP1D (Figure 4-C) at this condition show the high stability of this structure (Maximum RMSD in water is 1.4 Å). While the maximum RMSD of the CP1D without substitutions was 2.4 Å in water. Figure 4-D shows the Rg plots of the CP1D atoms in which lipid atoms were included. Inclusion of lipid atoms in Rg calculations confirms that lipid substitution makes the structure more compact in water than chloroform. Obtained RDFs of O$^{\cdots}$H (NH$^{\cdots}$OC) pairs for CP1D with lipid (Figure 5-A) show the first sharp peaks in water and chloroform were centered at r=1.85 Å, which this value is equal to the obtained value for CP1D without lipid in these solvents. The calculated amounts of the H-bonds of CP1D with lipid in water and chloroform during 50 ns were depicted in Figure 5-B. According to this figure, average number of H-bonds of CP1D with lipid substitution are 6 and 11 in water and chloroform, respectively. The amount of the H-bonds for CP1D (with/without lipid) in water is equal, which is in contrast to chloroform. The difference between the numbers of H-bond in water and chloroform shows the role of water on the inter-subunits H-bond formation. Since

water molecules form H-bond with the CO and NH groups of the CP1D, the number of the inter-subunits H-bond are reduced.

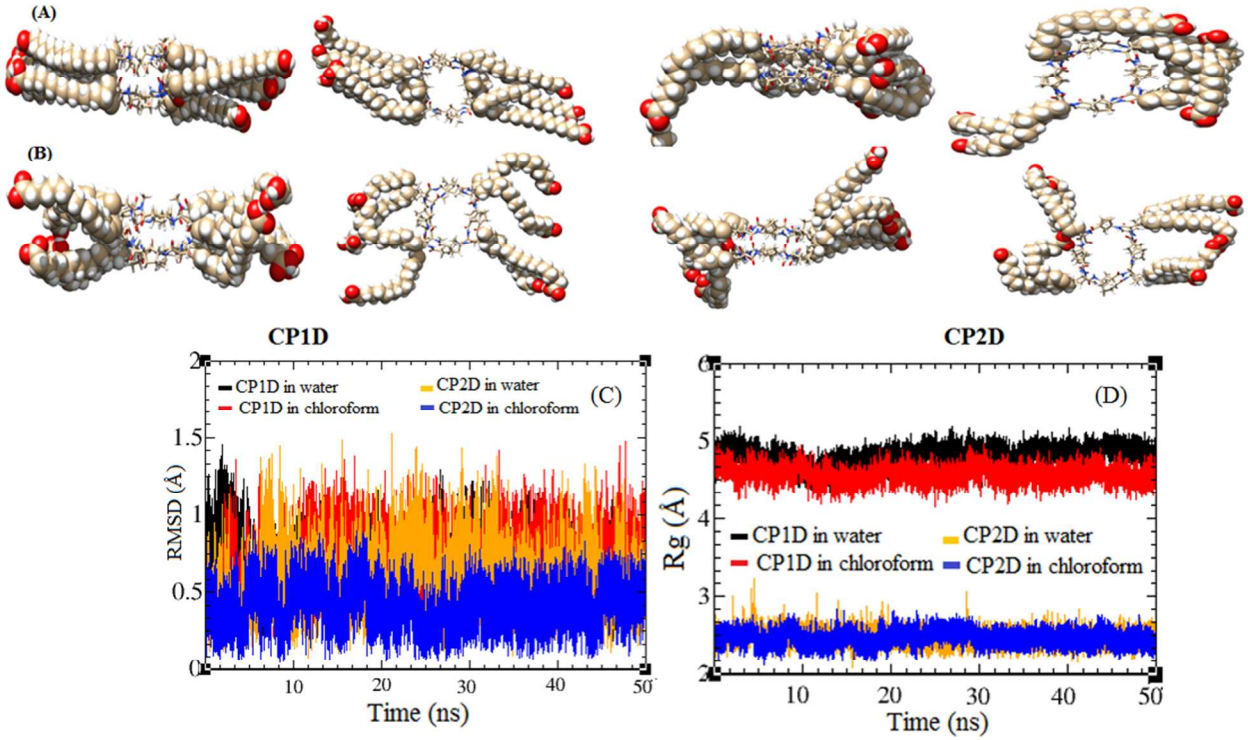

Figure 4. Obtained structures of the CP1D and CP2D (A) in water and (B) chloroform after 50 ns MD simulations. Calculated (C) RMSD and (D) Rg values of these structures in water and chloroform during the MD simulation (to have a better view, all structures were shown from the side and up views).

CP2D without lipid substitutions is not stable in water, while having a good stability in chloroform. Figure 4 shows the obtained tubular and stable structures of the CP2D with lipid in water and chloroform. Calculated RMSD (Figure 4-C) of the CP2D with lipid reveals the high stability of this structure because the maximum RMSD in water and chloroform is 1.5 and 0.8 Å, respectively. CP2D and CP1D with lipid show a similar behavior in polar solvents, these structures are

more compact in water because of the hydrophobic nature of the lipid substitutions. Comparison between the calculated Rg (Figure 4-D) of the CP1D and CP2D with lipid reveals that CP2D in both solvents is more compacted than CP1D.

A calculated average number of the H-bonds for CP2D with lipid are 6 and 13 in water and chloroform, respectively, which are higher than unsubstituted one by lipid. RDF calculations for O·····H (CO·····HN) pair of CP2D with lipid (Figure 5-A) show a sharp peak which is located at r=1.85 Å in both solvents, which is according to the substituted CP1D by lipid, too. These results indicate that lipid substitution stabilizes the dimer structures in polar and non-polar solvents.

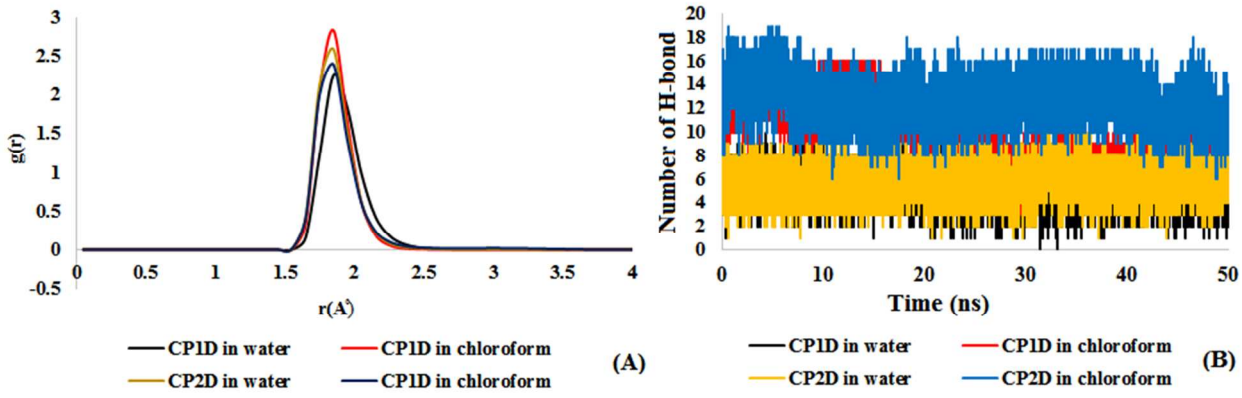

Figure 5. (A) RDF between the O and H atoms and (B) the calculated number of the H-bonds during the MD simulation of the CP1D and CP2D with lipid in different solvents.

To investigate the effect of lipid substitutions on the stability of the cyclic peptide nanotube, the behavior of the CPNT with lipid (CPNT2) was studied by

MD simulations in water and chloroform. Moreover the effect of the ionic structure of the lipid ($RCOO^-$) on the stability of CPNT, (CPNT3) have been studied, too.

Obtained structures of the CPNT2 after the 50 ns MD simulations in water (A) and chloroform (B) were shown in Figure 6. This figure shows that CPNT2 in both solvents is stable and has a tubular structure. CPNT1, the cyclic peptide without lipid substitutions in water is not stable (Figure 2), while lipid substitutions increase in the stability of the CPNT1 according to Figure 6. RMSD calculations (Figure 6-C) for CPNT2 reveal that this structure has more fluctuation in water than chloroform. Maximum RMSD in water is 5.5 Å which is low and acceptable. Because the lipid substitutions increase in the hydrophobic nature of the CPNT2, it will be more compact in water in comparison to other structures (Rg in Figure 6-D). RMSF plots (Figure 6-E) of the CPNT2 indicate that CPNT2 composed of 6 monomers is the most stable structure in water, in which the central monomers are more rigid than the terminal ones. An increase in the number of monomers of the CPNT2 in chloroform will not change the stability of this structure (according to Figure 6-E). According to Figure 6, chloroform molecules can be trapped inside the CPNT2 cavity.

Figure 7-B shows the number of the H-bonds of CPNT2 during the MD simulation in water and chloroform. According to this figure, the average number of the H-bonds in water and chloroform are 61 and 96, respectively. Showing that

chloroform made CPNT2 more stable than water. RDF plots (Figure 7-A) between O and H atoms of the monomers of CPNT2 show a sharp peak in water and chloroform at r=1.84 and 1.83 Å, respectively, confirming the H-bond formation between the CP units of the CPNT2.

The structures of the CPNT3 (Figure 6) after the 50 ns MD simulations in water and chloroform show a acceptable stability in the ionic form of lipid substitutions. RMSD calculations reveal that CPNT3 is more stable than CPNT2 in water (Figure 6-C). Also the calculated Rg of the CPNT3 are more than of CPNT2, it confirms that the CPNT2 is more compact in both solvents. RMSF values indicate that the CP units of the CPNT3 have the minimum fluctuation in chloroform, in comparison to the CPNT2 (Figure 6-E). According to Figure 7-B, the average number of the H-bonds of the CPNT3 in water and chloroform are 56 and 64, respectively, which are slightly lower than the number of inter-subunits H-bonds of CPNT2. The RDFs of the O and H atoms of the CP units of the CPNT3 (Figure 7-A) confirm that ionic form of the lipids has not important effect on the atomic distances, the RDF behavior of the CPNT3 is equal to the CPNT2 in the case of the O and H atoms. According to these results, ionic form of lipid substitutions has not an important effect on the stability of the CPNTs. For example, the calculated maximum RMSD of CPNT2 and CPNT3 in water are 5.5 and 5.0 Å, respectively, the small difference which is negligible. For comparison

of the CP dimers and CPNTs, the values of maximum of RMSD, Rg and average number of H-bonds summarized in Table 2. This table indicates that lipid substitutions increase the stability of CPNTs and dimers in the solution phase and increase in the number of H-bonds, elevates the CPNTs stability.

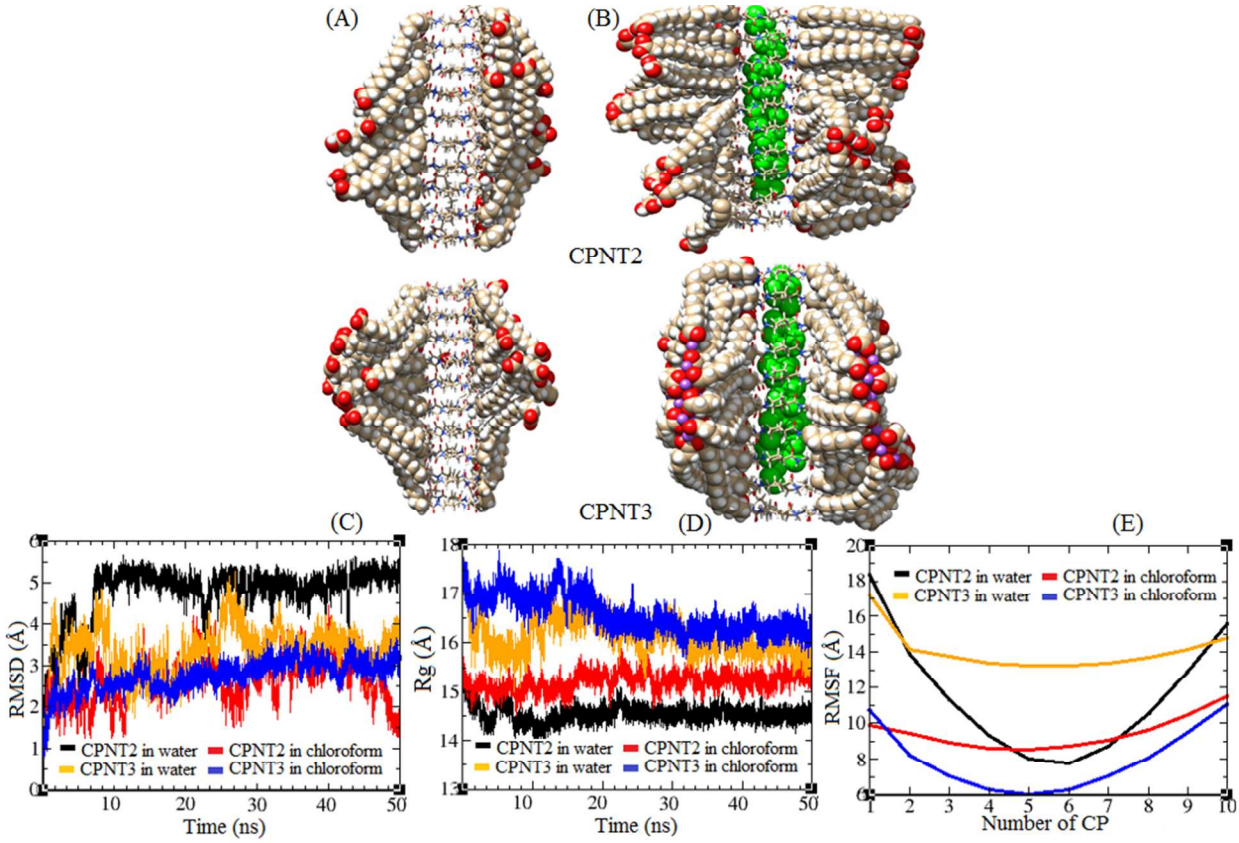

Figure 6. Obtained structures of CPNT2 and CPNT3 (A) in water and (B) chloroform after the 50 ns MD simulations. Calculated (C) RMSD, (D) Rg and (E) RMSF values of these structures during MD simulation.

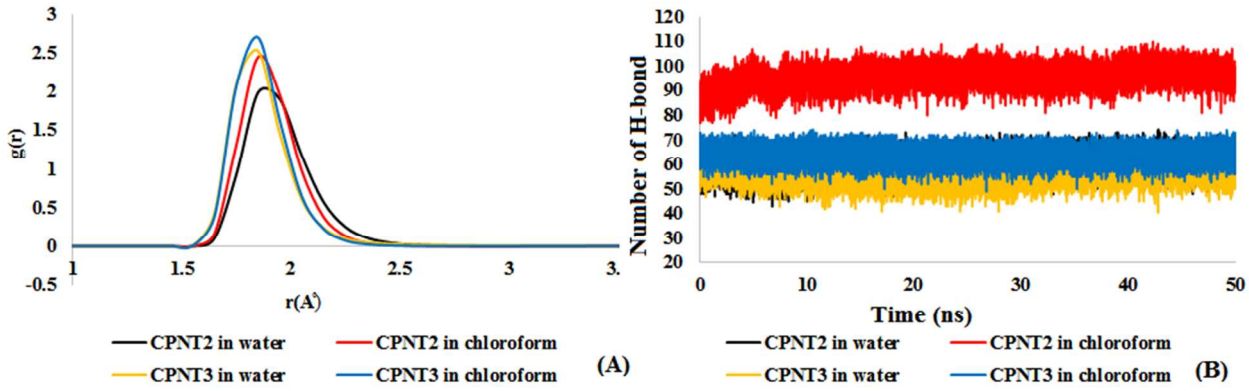

Figure 7. Calculated (A) RDF and (B) the number of the H-bonds of CPNT2 and CPNT3 in water and chloroform.

Table 2. Calculated maximum of RMSD and Rg (Å) and average number of H-bond of CP dimers and CPNTs in water and chloroform during the 50 ns MD simulations.

Structures	Solvents	Maximum of RMSD	Average number of H-bond	Maximum of Rg
CP1D	Water	2.4	6	8.14
	Chloroform	2.3	7	8.10
CP2D	Water	18.6	…..	19.70
	Chloroform	2.9	7	8.10
CP1D with lipid	Water	1.4	6	5.13
	Chloroform	0.9	11	4.80
CP2D with lipid	Water	1.5	6	2.62
	Chloroform	0.8	13	2.64
CPNT1	Water	12.3	45	20.92
	Chloroform	1.6	62	15.60
CPNT2	Water	5.5	61	15.40
	Chloroform	4.1	96	15.80
CPNT3	Water	5.0	56	17.80
	Chloroform	3.2	64	17.90

Application of the CPNT with and without lipid substitution as a molecular channel in DMPC bilayer

Based on the good stability obtained from the MD simulations on the CPNTs (with/without lipid substitutions) in solution, it is reasonable to be used as a molecular container. Therefore, to investigate the application of CPNTs as a molecular channel, CPNTs were inserted in the center of fully hydrated DMPC bilayer and their behavior were investigated during the 50 ns MD simulations (Figure 8). Analysis of the CPNT1 in DMPC bilayer indicates that this structure composed of 10 CP monomers is stable for 35 ns. After 35 ns two terminal CPs

were separated from the CPNT1, while residual CPs in DMPC bilayer make a stable channel. RMSD and Rg calculation (Figure 8-C and D) confirm this behavior. Figure 8 shows structure of CPNT3 inside DMPC bilayer after 50 ns MD simulations, which is a stable molecular channel. RMSD, RMSF and Rg calculations of CPNT3 reveal the high stability of this structure in DPMC bilayer. Calculated average number of H-bonds of the CPNT1 and CPNT3 inside the DMPC membrane are 46 and 55, respectively. RDF calculation reveals that O···H distance in the CPNTs is 1.8 Å for H-bond formation in DMPC membrane. Figure 9 shows water molecules and K^+ ions inside the CPNT3 at 5, 15 and 25 ns after simulation (in this figure DMPC bilayer has been omitted for clarity). According to Figure 9, CPNT3 has a tubular structure and work as a molecular channel inside the DMPC bilayer. These results indicate that these CPNTs with and without lipid substitutions have stable nanotubular structure in membrane and can be used as a molecular channel for transmission small molecules across the cell membrane.

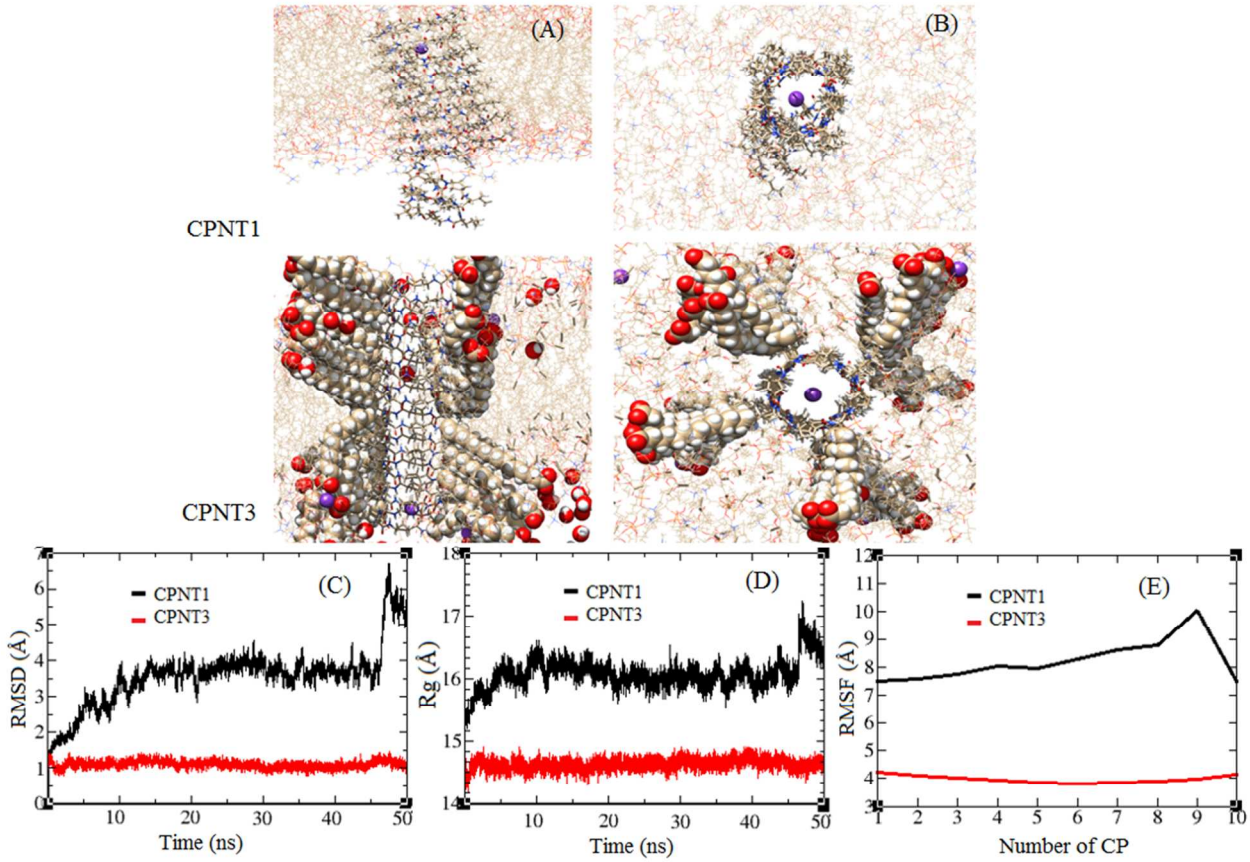

Figure 8. Obtained structure of CPNT1 and CPNT3 in DMPC bilayer that is shown from (A) side and (B) up views after 50 ns in MD simulations. Calculated (C) RMSD, (D) Rg and (E) RMSF of these structures during the simulations.

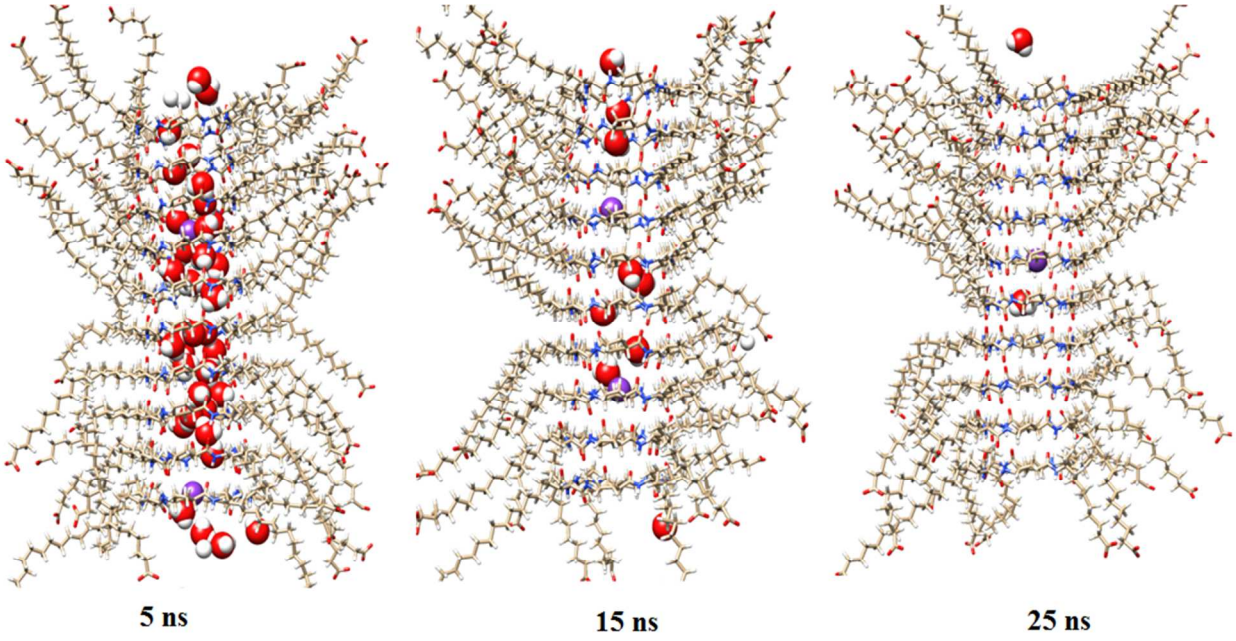

Figure 9. The structures of the CPNT3 in DMPC bilayer during the simulation.

MM-PBSA and MM-GBSA binding energies

MM-PBSA (PB) and MM-GBSA (GB) calculations were done to obtain the free energy of binding for the addition of each CP monomer (with/without lipid substitutions) to other CP units. According to Table 3, lipid substitutions slightly increase the van der Waals energy (ΔE_{vdW}) in water and chloroform, because of their hydrophobic nature. The contribution of the electrostatic energy (ΔE_{ele}) for CPNTs in chloroform is more than water, because of the higher number of inter-subunits H-bonds in chloroform. Comparison between the values of non-polar contribution energy (ΔE_{np}) of the CPNT with and without lipid, confirms that non-polar substitutions increase ΔE_{np} in both solvents. Solvation free energy (ΔG_{sol}) for

both of the CPNT (with/without lipid) in water is more than chloroform, in agreement with a lower stability of the CPNTs in water as a polar solvent.

Table 3. Calculated contributions of the energy components (kcal mol^{-1}) for addition of the CP unit to other CPs from the PB method in water and chloroform for CPNT (with/without lipid substitutions).

	CP2	CP3	CP4	CP5	CP6	CP7	CP8	CP9	CP10
Without lipid substitution									
water									
ΔE_{vdW}	-26.78	-27.73	-28.61	-28.90	-28.42	-0.01	-0.01	-28.09	-27.06
ΔE_{ele}	-8.25	-6.51	-8.56	-8.02	-6.94	0.02	0.01	-8.12	-8.26
ΔE_{PB}	8.61	7.73	9.18	9.55	9.58	0.00	0.00	8.91	8.43
ΔE_{np}	-31.63	-32.29	-31.28	-29.24	-26.81	0.57	0.56	-30.57	-31.35
ΔG_{gas}	-35.03	-34.24	-37.17	-36.92	-35.36	0.01	0.01	-36.21	-35.32
ΔG_{sol}	19.25	20.74	22.91	23.93	25.02	0.58	0.59	20.83	19.99
chloroform									
ΔE_{vdW}	-30.14	-30.33	-29.41	-32.16	-29.43	-0.01	-0.01	-30.64	-29.35
ΔE_{ele}	-8.60	-8.45	-8.34	-8.74	-7.87	0.01	0.01	-8.18	-8.34
ΔE_{PB}	7.10	7.36	7.87	7.90	8.04	0.01	0.01	7.10	6.92
ΔE_{np}	-29.70	-30.89	-31.09	-29.36	-26.96	0.57	0.57	-29.74	-31.02
ΔG_{gas}	-38.74	-38.78	-37.76	-40.91	-37.31	0.01	0.00	-38.82	-37.69
ΔG_{sol}	19.08	20.98	21.95	22.48	23.52	0.59	0.59	19.10	18.66
With lipid substitution									
water									
ΔE_{vdW}	-83.45	-75.27	-87.46	-80.94	-64.92	-79.29	-68.02	-65.27	-59.27
ΔE_{ele}	-5.59	-7.58	-4.04	-7.10	-6.63	-5.91	-6.20	-6.81	-6.66
ΔE_{PB}	9.62	10.25	9.17	10.49	10.00	10.10	10.19	10.14	10.65
ΔE_{np}	-77.92	-68.43	-77.19	-72.47	-59.76	-69.45	-61.80	-60.08	-53.96
ΔG_{gas}	-89.05	-82.84	-91.50	-88.04	-71.54	-85.20	-61.79	-72.08	-65.94
ΔG_{sol}	28.63	41.39	35.16	40.04	47.18	40.66	46.76	46.53	50.16
Chloroform									
ΔE_{vdW}	-83.90	-75.07	-89.50	-82.12	-65.46	-78.76	-66.27	-63.06	-55.84
ΔE_{ele}	-5.96	-7.52	-3.41	-7.08	-6.74	-6.97	-5.80	-7.45	-6.61
ΔE_{PB}	7.87	8.25	7.33	8.07	7.96	8.29	8.09	8.37	8.15
ΔE_{np}	-78.06	-68.13	-77.33	-71.08	-59.43	-68.88	-59.44	-57.86	-51.79
ΔG_{gas}	-89.86	-82.59	-92.91	-89.21	-72.20	-85.74	-72.07	-70.51	-62.45
ΔG_{sol}	26.53	38.91	32.76	38.37	45.18	38.59	46.16	45.70	48.55

Calculated free energy of binding (ΔG_{bin}), using PB and GB methods, for CPNTs (with/without lipid substitutions) in water and chloroform with its standard deviation (SD) reported in Table 4. According to Table 4, both of the GB and PB

methods confirm that lipid substitutions increase in the stability of CPNT. Moreover, the CPNT without lipid has bigger ΔG_{bin} in chloroform, because of the higher number of inter-subunits H-bond, in agreement with the obtained results in the previous sections. While the values of ΔG_{bin} of the CPNT with lipid substitutions have not important difference in water and chloroform. The remarkable point is that the hydrophobic lipid side chains elevate the ΔG_{bin} in the polar environment. Linear correlation between the number of the CP monomers and ΔG_{bin} (Figure 10) shows that increase the length of the CPNTs reduces the stability.

Table 4. Calculated total free energy of binding (kcal mol^{-1}) for the addition of the CP unit (with/without lipid substitutions) to other CPs in water and chloroform using the PB and GB methods.

	water				chloroform			
	Without lipid substitution		With lipid substitution		Without lipid substitution		With lipid substitution	
Number of CP units	ΔG	SD	ΔG	SD	ΔG	SD	ΔG	SD
				GB method				
2	-30.88	2.93	-92.12	1.96	-34.11	1.51	-92.58	2.05
3	-30.80	2.77	-83.49	2.59	-34.36	1.97	-83.29	2.19
4	-32.61	2.62	-94.15	2.14	-33.28	2.56	-95.84	1.95
5	-32.56	2.26	-88.72	2.69	-36.27	1.36	-89.94	2.12
6	-31.31	1.68	-71.10	2.32	-32.69	1.83	-71.68	1.69
7	-0.01	0.00	-86.58	2.19	-0.01	0.00	-86.29	2.38
8	-0.01	0.00	-74.32	2.40	-0.00	0.00	-72.00	1.73
9	-32.01	2.19	-72.11	1.76	-34.34	1.74	-69.65	1.44
10	-31.31	2.03	-64.87	1.63	-33.62	2.50	-61.00	1.38
				PB method				
2	-15.79	2.72	-60.42	1.96	-19.66	1.43	-63.33	1.96
3	-13.50	2.62	-41.45	3.10	-17.80	1.83	-43.68	2.48
4	-14.25	2.61	-56.35	2.24	-15.80	2.56	-60.15	2.20
5	-12.99	2.18	-48.00	2.97	-18.43	1.45	-50.84	2.44
6	-10.33	1.63	-24.37	2.62	-13.79	1.75	-27.02	1.91
7	0.59	0.00	-44.54	2.67	0.60	0.00	-47.15	2.61
8	0.59	0.00	-27.47	2.77	0.60	0.00	-25.91	1.90
9	-15.38	2.10	-25.54	2.02	-19.72	1.65	-24.82	1.70

10	-15.33	1.88	-15.77	2.03	-19.03	2.23	-13.90	1.75

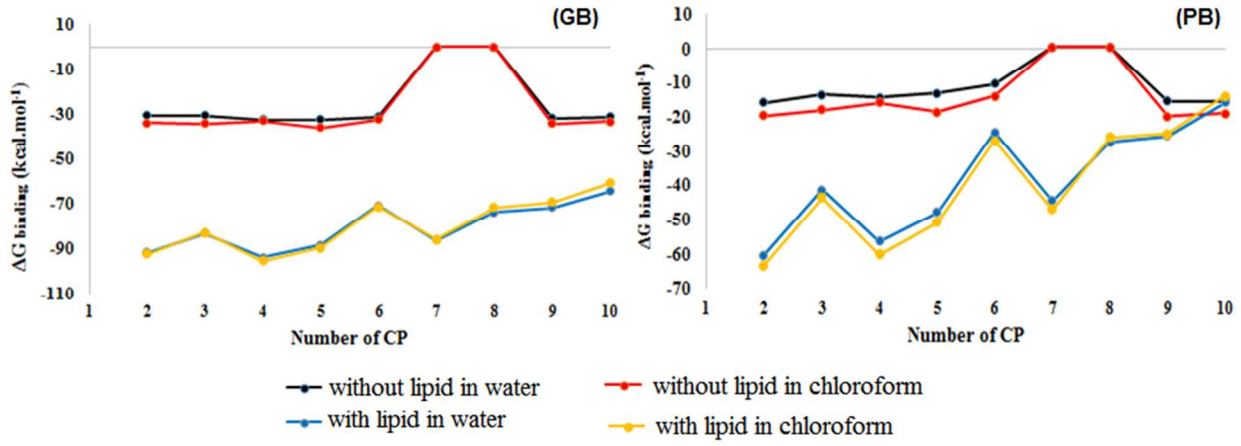

Figure 10. The relationship between the number of the CP units and the calculated ΔG_{bin} using the PB and GB method in water and chloroform.

Structural, IR vibrational frequency and energy analysis by DFT method

In order to have a better insight into the studied system from the quantum chemistry aspects, density functional theory (DFT) calculations were done on the CP1, CP2 and their dimers in the gas phase, water and chloroform. Optimized structures of the monomers and dimers of the CP1 and CP2 in the gas phase were shown in Figure S2. Calculated geometrical parameters of the CP1, CP2 monomers and their dimers were reported in Table S1 (experimental parameters of CP2 monomer and its dimer is not avalibale[28]). According to this table, the theoretical structural parameters are in good agreement with the experimental ones. Calculated C=O and N—H bond lengths of the monomer are 1.23 and 1.01 Å in the gas phase,

respectively, while the corresponding lengths of the dimer are 1.24 and 1.02 Å, respectively. Calculated C=O bond length of CP1D and CP2D is 1.24 Å which is according to the experimental value, 1.21 Å. Moreover, the calculated N⋯O distance in the CP1D and CP2D are 2.93 and 2.95 Å, respectively, which is equal to the experimental value of 2.93 Å. The average calculated angles of NCO of CP1D and CP2D are 122.90˚ and 122.56˚ which is according to the experimental value of 122.91˚, too. Table 5 shows the calculated IR vibrational frequencies of N—H and C=O bond lengths in the gas phase, water and chloroform. Comparison between the calculated frequencies of C=O and N—H bonds of the monomer and dimers indicates that the dimerization process has an important effect on the IR vibrational modes. Vibrational frequencies of the N—H bond of CP1 and CP2 monomers showed a red shift in polar solvent. Moreover N—H vibrational frequency of the CP1 and CP2 showed a blue shift during the dimerization process in the gas phase, water and chloroform. The vibrational frequency of the C=O bonds of CP1 and CP2 represented a blue shift during the dimerization, too. Moreover, solvent reduces the calculated vibrational frequencies of the C=O bonds of CP1D and CP2D in comparison to the gas phase.

Table 5. Calculated IR vibrational frequencies (cm^{-1}) of CP monomers and dimers in the gas phase, water and chloroform.

		CP1			CP2		
Bond	**structure**	**Gas**	**Water**	**Chloroform**	**Gas**	**Water**	**Chloroform**
N—H	**Monomer**	3646.11	3660.71	3654.60	3650.49	3686.53	3649.06
	Dimer	3515.23	3523.96	3524.56	3558.87	3577.50	3577.58
C=O	**Monomer**	1779.56	1741.23	1750.39	1809.10	1799.06	1801.38

Dimer	1739.99	1724.30	1728.58	1782.58	1773.73	1776.79

Calculated ΔG for CP1D in the gas phase, water and chloroform are -41.4, -20.40 and -28.2 kcal mol^{-1} and for CP2D are -42.5, -32.2 and -28.7 kcal mol^{-1}, respectively. These values are more than calculated by molecular mechanic methods (PB and GB). Accordingly the dimerization is more favorable in the gas phase than the solution. Additionally, CP1D is more stable in chloroform than water, which is in agreement with MD simulation.

Quantum reactivity indices and NBO analysis

Quantum reactivity indices[61,62] such as electronic chemical potential (μ), chemical hardness (η) and global electrophilicity index (ω), have been calculated and reported in Table 6. According to Table 6, through the dimerization process, band gap or chemical hardness was depleted while the chemical potential and electrophilicity index were elevated. Since the calculated η of the CP2D is more than CP1D, reactivity of CP1D is bigger than CP2D. According to an analysis of the HOMO and LUMO orbitals of the CP dimers it is confirmed that they are located on the C=O and N—H groups, respectively, confirming the major interactions between the CP unit of the dimers are due to the N—H···O=C molecular orbital interactions.

Table 6. Calculated orbital energies and quantum reactivity indices of the CP monomers and dimers in the gas phase, water and chloroform.

	Structures	CP1					CP2				
		$-E_{HOMO}$	E_{LUMO}	$-\mu$	η	$10^2\omega$	$-E_{HOMO}$	E_{LUMO}	$-\mu$	η	$10^2\omega$
Gas	Monomer	0.299	0.062	0.119	0.361	1.96	0.307	0.067	0.120	0.347	1.93
	Dimer	0.297	0.051	0.123	0.348	2.17	0.305	0.050	0.128	0.355	2.31
Water	Monomer	0.301	0.058	0.122	0.359	2.07	0.310	0.063	0.124	0.373	2.06
	Dimer	0.303	0.045	0.129	0.348	2.39	0.308	0.047	0.131	0.355	2.42
Chloroform	Monomer	0.301	0.059	0.121	0.360	2.03	0.309	0.064	0.123	0.373	2.03
	Dimer	0.301	0.047	0.127	0.348	2.32	0.307	0.047	0.130	0.354	2.39

The calculated atomic charges of O and H atoms of the CP monomers and the dimers in the gas phase, water and chloroform have been reported in Table S2. During the dimerization negative and positive charges of O and H atoms, were increased respectively. And the polar solvent reduces the charge changes during the dimerization which indicates that polar solvent reduces the O$^{\cdots}$H interaction.

Table 7 shows the calculated donor-acceptor orbital interaction energies, E(2), between the lone pair electron of O atoms with antibonding molecular orbitals of N—H bonds ($\sigma^*_{N—H}$). According to Table 7, CP1 units have stronger orbital interactions with each other in comparison to the CP2 units. For example, the interaction energies of the Lp_{O3} and $\sigma^*_{N1—H2}$ of CP1D are 14.7, 14.8 and 14.8 kcal mol^{-1} in the gas phase, water and chloroform, respectively, while the corresponding interactions of CP2D in these media are 7.4, 7.40 and 7.4 kcal mol^{-}

[1], respectively. Stronger orbital interactions of the CP1D make it more stable than CP2D, which is in agreement with MD results. O atoms of the CP1D have stronger interaction with $\sigma^*_{N—H}$ in the solvents in comparison to the gas phase, while in the case of CP2 monomer of the dimer structure, the corresponding orbital interactions have been reduced in the solvent.

Table 7. Significant natural bond orbital interactions between the two CPs in the gas phase, water and chloroform and their second-order perturbation stabilization energies E(2) (kcal mol^{-1}).

	CP1D			CP2D		
	Gas	**Water**	**Chloroform**	**Gas**	**Water**	**Chloroform**
$LpO_3 \rightarrow \sigma^*_{N1—H2}$	14.7	14.8	14.8	7.4	7.4	7.4
$LpO_6 \rightarrow \sigma^*_{N8—H7}$	13.2	13.3	13.3	8.3	8.2	8.2
$LpO_{11} \rightarrow \sigma^*_{N9—H10}$	14.7	14.8	14.8	8.3	8.2	8.2
$LpO_{14} \rightarrow \sigma^*_{N16—H15}$	13.2	13.3	13.3	7.4	7.4	7.4
$LpO_{19} \rightarrow \sigma^*_{N17—H18}$	14.7	14.8	14.8	7.4	7.4	7.4
$LpO_{22} \rightarrow \sigma^*_{N24—H23}$	13.2	13.3	13.3	8.3	8.2	8.2
$LpO_{27} \rightarrow \sigma^*_{N25—H26}$	14.7	14.8	14.8	7.4	7.4	7.4
$LpO_{30} \rightarrow \sigma^*_{N32—H31}$	13.2	13.3	13.3	8.3	8.2	8.2

LOL, ELF and electron density analysis

Quantum theory of atoms in molecules (QTAIM) analysis at different characteristic points, particularly at the bond critical points (BCP) of O···H bonds for the CP dimers has been performed in the gas phase and solutions. Topological analyses of the O···H bonds are reported in Table 8. According to this table, increase in the electron density (ρ), increases the O···H interaction. Calculated values of electron density of CP1D are bigger than CP2D, which indicate a stronger interaction for O···H in CP1D and its higher stability. Calculated positive values of ∇^2 (Laplacian) for CP1D and CP2D, reveal the electrostatic interactions

of the O and H atoms. The nature of the interaction, covalent or non-covalent, can be determined by using the ratio of the kinetic energy density (G) to the potential energy density (V). According to Table 8, the -G/V ratios of CP1D and CP2D are near to 1.0 and confirms the non-covalent nature of the interaction between the O and H atoms of the dimers in the gas and solution phases. Figure 11 shows the ELF, LOL and electron density diagrams for NH⋯O=C interactions of the dimers. Large and small values of these parameters at the BCP show covalent and electrostatic interaction, respectively. According to Figure 11, electron density, LOL and ELF values of the O⋯H bonds are small and confirms their electrostatic interaction in the CP dimers.

Table 8. Calculated topological parameters (in a.u) of the O⋯H interaction at the BCP in the gas and solution phases for CP dimers.

		CP1D			CP2D		
	Parameters	**Gas**	**Water**	**Chloroform**	**Gas**	**Water**	**Chloroform**
N1H2⋯O3	**ρ**	0.028	0.029	0.029	0.025	0.025	0.025
	$\nabla^2_{(\rho)}$	0.099	0.099	0.099	0.080	0.080	0.080
	-G/V	0.988	0.984	0.984	0.963	0.963	0.963
N8H7⋯O6	**ρ**	0.026	0.026	0.026	0.026	0.026	0.026
	$\nabla^2_{(\rho)}$	0.087	0.087	0.087	0.086	0.086	0.086
	-G/V	0.982	0.982	0.982	0.970	0.970	0.969
N9H10⋯O11	**ρ**	0.028	0.029	0.029	0.025	0.025	0.025
	$\nabla^2_{(\rho)}$	0.099	0.099	0.099	0.080	0.080	0.080
	-G/V	0.988	0.984	0.984	0.962	0.963	0.963
N15H16⋯O14	**ρ**	0.026	0.026	0.026	0.026	0.026	0.026
	$\nabla^2_{(\rho)}$	0.087	0.087	0.087	0.086	0.086	0.086
	-G/V	0.982	0.982	0.982	0.970	0.970	0.969
N17H18⋯O19	**ρ**	0.028	0.029	0.029	0.025	0.025	0.025
	$\nabla^2_{(\rho)}$	0.099	0.099	0.099	0.080	0.080	0.080
	-G/V	0.988	0.984	0.984	0.963	0.963	0.963
N24H23⋯O22	**ρ**	0.026	0.026	0.026	0.026	0.026	0.026
	$\nabla^2_{(\rho)}$	0.087	0.087	0.087	0.086	0.086	0.086
	-G/V	0.982	0.982	0.982	0.970	0.969	0.969
N25H26⋯O27	**ρ**	0.028	0.029	0.029	0.025	0.025	0.025
	$\nabla^2_{(\rho)}$	0.099	0.099	0.099	0.080	0.080	0.080

	-G/V	0.988	0.984	0.984	0.963	0.963	0.963
	ρ	0.026	0.026	0.026	0.026	0.026	0.026
N32H31···O30	$\nabla^2_{(\rho)}$	0.087	0.087	0.087	0.086	0.086	0.086
	-G/V	0.982	0.982	0.982	0.970	0.969	0.969

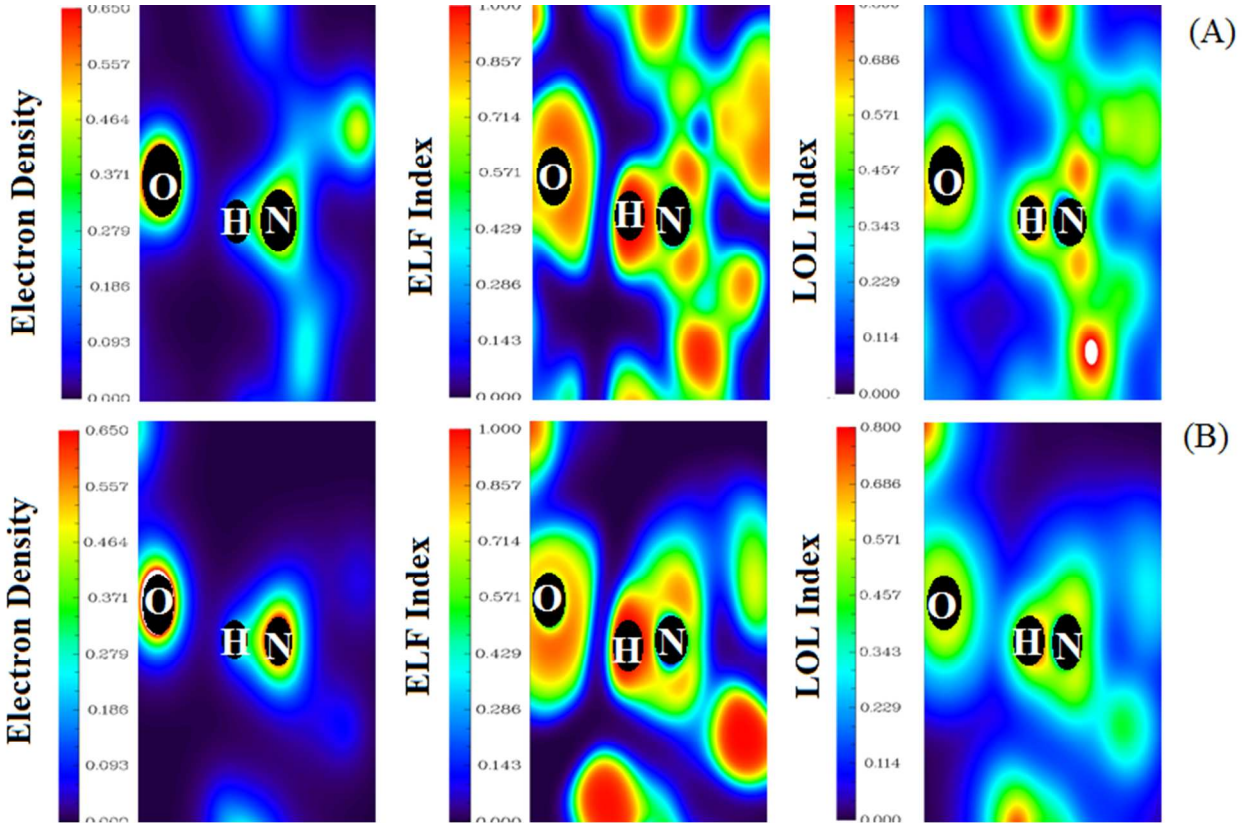

Figure 11. Electron density, ELF and LOL diagrams of the C=O····HN interaction of (A) CP1D and (B) CP2D in the gas phase.

Conclusion

50 ns MD simulations on the CP1D, CP2D and CPNTs in the water and chloroform reveal that these structures are more stable in chloroform than water. During the simulation, chloroform molecules diffuse inside the cavity of the CPNTs and this shows that CPNTs are good container for non-polar small

molecules. Lipid substitutions have a significant effect on the stability of the CP dimers and CPNT in the polar and non-polar solvents. MM-PBSA and MM-GBSA calculations reveal that increase in the length of the CPNTs, reduces their stability. Dynamical behavior of the CPNT with lipid substitutions in fully hydrated DMPC bilayer shows that this structure is a good molecular channel across the membrane.

DFT calculations on the structures of the CP1, CP2 monomers and their dimers in the gas phase and two solvents, reveal that CP1D are more stable than CP2D. HOMO-LUMO analysis indicates that the dimer formation is due to molecular orbital interactions between the C=O and NH groups of the CP units of the dimers. QTAIM analysis confirmed H-bond formation between the CP monomers electrostatic nature of the O⋯⋯H interaction.

Acknowledgement

Research Council of Ferdowsi University of Mashhad is acknowledged for financial supports (Grant No. 3/32435, 1393/8/17). We hereby acknowledge that part of this computation was performed on the HPC center of Ferdowsi University of Mashhad.

References

1 M. R. Ghadiri, J. R. Granja, R. A. Milligan, D. E. McRee and N. Khazanovich, *Nature,* 1993, **366**, 324.

2 M. R.Ghadiri, J. R. Granja and L. K. Buehler, *Nature* 1994, **369**, 301.

3 M. R. Ghadiri, K. Kobayashi, J. R. Granja, R. K. Chadha, and D. E. McRee, *Angew. Chem., Int. Ed. Engl*., 1995, **34**, 93.

4 K. Motesharei and Ghadiri, *J. Am. Chem. Soc*., 1997, **119**, 11306.

5 H. S. Kim, J. D. Hartgerink and M. R. Ghadiri, *J. Am. Chem. Soc.,* 1998, **120**, 4417.

6 J. D. Hartgerink, T. D. Clark and M. R. Ghadiri, *Chem. Eur. J.,* 1998, **4**, 1367.

7 J. Sánchez-Quesada, H. S. Kim and M. R. Ghadiri, *Angew. Chem., Int. Ed*., 2001, **40**, 2503.

8 S. Fernandez-Lopez, H. S. Kim, E. C. Choi, M. Delgado, J. R. Granja, A. Khasanov, K. Kraehenbuehl, G. Long, D. A. Weinberger, K. M. Wilcoxen and M. R. Ghadiri, *Nature*, 2001, **412**, 452.

9 W. S. Horne, N. Ashkenasy and M. R. Ghadiri, *Chem. Eur. J.* 2005, **11**, 1137.

10 A. Ortiz-Acevedo H. Xie, V. Zorbas, W. M. Sampson, A. B. Dalton, R. H. Baughman, R. K. Draper, I. H. Musselman and G. R. Dieckmann, *J. Am. Chem. Soc.,* 2005, **127**, 9512.

11 C. R. Martin and P. Kohli, *Nat. Rev. Drug Discovery*, 2003, **2**, 29-37.

12 X. Gao and H. Matsui, *Adv. Mater.,* 2005, **17**, 2037.

13 V. Dartois, J. Sanchez-Quesada, E. Cabezas, E. Chi, C. Dubbelde, C. Dunn, C. Gritzen, D. Weinberger, J. R. Granja, M. R. Ghadiri and T. R. Parr, *Antimicrob. Agents Chemother*., 2005, **49**, 3302.

14 N. Ashkenasy, W. S. Horne and M. R. Ghadiri, *Small*, 2006, **2**, 99.

15 R. de la Rica, C. Pejoux and H. Matsui, *Adv. Funct. Mater.* 2011, **21**, 1018.

16 T. Xu, N. Zhao, F. Ren, R. Hourani, M. Tsang Lee, J. Y. Shu, S. Mao and B. A. Helms, *ACS Nano,* 2011, **2**, 1376.

17 M. Mizrahi, A. Zakrassov, J. Lerner-Yardeni and N. Ashkenasy, *Nanoscale,* 2012, **4**, 518.

18 H. Liu, J. Chen, Q. Shen, W. Fu and W. Wu, *Mol. Pharm.,*2010, **7**, 1985.

19 R. Vijayaraj, S. V. Damme, P. Bultinck and V. Subramanian, *Phys. Chem. Chem. Phys.,* 2013, **15**, 1260.

20 C. Appelt, A. Wessolowski, J. Arvid Soderhall, M. Dathe and P. Schmieder, *ChemBioChem,* 2005, **6**, 1654.

21 H. Hwang, G. C. Schtaz and M. A. Ratner, *J. Phys. Chem. A*, 2009, **113**, 4780.

22 Stein,W.D.Channels, Carriers, and Pumps: An Introduction to Membrane Transport; Academic Press: *San Diego, CA,* 1990.

23 R. Gracia-Fandino, M. Amorin, L. Castedo and J. R. Granja, *Chem. Sci,* 2012, **3**, 3280.

24 M. Izadyar, M. Khavani and M. R. Housaindokht, *Phys. Chem. Chem. Phys.,* 2015, **17**, 11382.

25 R. Vijayaraj, S. V. Damme, P. Bultinck and V. Subramanian, *Phys. Chem. Chem. Phys.,* 2012, **14**, 15135.

26 R. Gracia-Fandini and R. Granja Guillan, *J. Phys. Chem. C*, 2013, **117**, 10143.

27 H. S. Kim, J. D. Hartgerink and M. R Ghadiri, *J. Am. Chem. Soc.,* 1998, **120,** 4417.

28 R. J. Brea, L. Castedo and J. R. Granja, *Chem. Commun.,* 2007, **31**, 3267.

29 W. L. Jorgensen*, J. Am. Chem. Soc.,* 1981, **103,** 335.

30 W. L. Jorgensen, J. Chandrasekhar, J. D. Madura, R. W. Impey and M. L. Klein*, J. Chem. Phys.,* 1983, **79**, 926.

31 P. Cieplak, J. Caldwell and P. Kollman, *J. Comput. Chem.,* 2001, **22**, 1048.

32 J. Wang, W. Wang, P. A. Kollman and D. A. Case, *J. Mol. Graphics Modell.*, 2006, **25,** 247.

33 B. P. Uberuaga, M. Anghel and A. F. Voter, *J. Chem. Phys.,* 2004, **120,** 6363.

34 D. J. Sindhikara, S. Kim, A. F. Voter and A. E. Roitberg, *J. Chem. Theory Comput.,* 2009, **5**, 1624.

35 J. P. Ryckaert, G. Ciccotti and H. J. C. Berendsen, *J. Comput. Phys.,* 1977, **23**, 327.

36 U. Essman, L. Perera, M. Berkowitz, T. Darden, H. Lee and L. Pedersen, *J. Chem. Phys.,* 1995, **103**, 8577.

37 D. A. Case, T. A. Darden, T. E. Cheatham, C. L. Simmerling, J. Wang, R. E. Duke, R. Luo, R. C. Walker, W. Zhang, K. M. Merz, B. Roberts, S. Hayik, A. Roitberg, G. Seabra, J. Swails, A. W. Go¨tz, I. Kolossva´ry, K. F. Wong, F. Paesani, J. Vanicek, R. M. Wolf, J. Liu, X. Wu, S. R. Brozell, T. Steinbrecher, H. Gohlke, Q. Cai, X. Ye, J. Wang, J. Hsieh, G. Cui, D. R. Roe, D. H. Mathews, M. G. Seetin, R. Salomon-Ferrer, C. Sagui, V. Babin, T. Luchko, S. Gusarov, A. Kovalenko and P. A. Kollman, AMBER 12, University of California, San Francisco, 2012.

38 C. J. Dickson, L. Rosso, R. M. Betz, R. C. Walker and I. R. Gould, *Proteins,* 2012, **8**, 9617.

39 C. J. Dickson, B. D. Madej, A. A. Skjevik, R. M. Betz K. Teigen, I. R. Gould and R. C. Walker, *J. Chem. Theory Comput.,* 2014, **10**, 865.

40 J. Wang, R. M. Wolf, J. W. Caldwell, P. A. Kollamn and D. A. Case, J. *Comput. Chem.,* 2004, **25**, 1157.

41 http://www.ambermd.org.

42 R. Bill, T. D. McGee, J. M. Swails, N. Homeyer, H. Gohlke and A. E. Roitberg, *J. Chem. Theory Comput.,* 2012, **8**, 3314.

43 H. Gohlke, C. Kiel and D. A. Case, *J. Mol. Biol.,* 2003, **330**, 891.

44 J. Srinivasan, T. E. Cheatham, P. Cieplak, P. A. Kollman and D. A. Case, *J. Am. Chem. Soc.,* 1998, **120**, 9401.

45 Y. Zhao and D. G. Truhlar, *J. Phys. Chem.,* 2006, **110**, 5121.

46 R. J. Bartlett and G. D. Purvis, *Int. J. Quantum Chem.,* 1978, **14**, 561.

47 M. J. Frisch, G. W. Trucks, H. B. Schlegel, G. E. Scuseria, M. A. Robb, J. R. Cheeseman, J. A. Montgomery, T. Vreven, K. N. Kudin and J. C. Burant, et al., Gaussian 09, Gaussian, Inc., Pittsburgh, PA, 2009.

48 M. Cossi, N. Rega, G. Scalmani and V. Barone, *J. Comput. Chem.,* 2003, **24**, 669.

49 M. Cossi, V. Barone, R. Cammi and J. Tomasi, *Chem. Phys. Lett.*, 1996, **255**, 327.

50 A. E. Reed, L. A. Curtiss and F. Weinhold, *Chem. Rev.,* 1988, **88**, 899.

51 R. F. W. Bader, Atoms in Molecules, A Quantum Theory, Oxford University Press, New York, 1990.

52 R. F. W. Bader, *Chem. Rev.,* 1991, **91**, 893.

53 W. Scherer, P. Sirsch, D. Shorokhov, M. Tafipolsky, G. S. McGrady and E. Gullo, *Chem. Eur. J.,* 2003, **9**, 6057.

54 A. Shurki, P. C. Hiberty and S. Shaik, *J. Am. Chem. Soc.,* 1999, **121**, 822.

55 A. D. Becke and K. E. Edgecombe, *J. Chem. Phys.,* 1990, **92**, 5397.

56 A. Savin, R. Nesper, S. Wengert and T. Fassler, *Angew. Chem., Int. Ed. Engl.,* 1997, **36,** 1808.

57 J. K. Burdett and T. A. McCormick, *J. Phys. Chem. A,* 1998, **102**, 6366.

58 A. Savin, V. Jepsen, J. Flad, O. K. Andersen, H. Preuss and H. G. von Schnering, *Angew. Chem., Int. Ed. Engl.*, 1992, **31**, 187.

59 V. Tsirelson and A. Stash, *Chem. Phys. Lett.,* 2002, **351**, 142.

60 T. Lu and W. Chen, *J. Comput. Chem.,* 2012, **33**, 580.

61 M. Izadyar, M.Gholizadeh, M. Khavani and M. R. Housaindokht, *J. Phys. Chem. A,* 2013, **117**, 2427.

62 M. Izadyar and M. Khavani*, Int. J. Quantum Chem.,* 2014, **114**, 1.